International Journal of Mechanical Sciences 53 (2011) 98–107

Contents lists available at ScienceDirect

International Journal of Mechanical Sciences

journal homepage: www.elsevier.com/locate/ijmecsci

Transport properties in fibrous elastic rhombic composite with imperfect contact condition

Juan C. López-Realpozo [a], Reinaldo Rodríguez-Ramos [a,*], Raúl Guinovart-Díaz [a], Julián Bravo-Castillero [a], Federico J. Sabina [b]

[a] Facultad de Matemática y Computación, Universidad de La Habana, San Lázaro y L, Vedado, Habana 4, CP-10400, Cuba
[b] Instituto de Investigaciones en Matemáticas Aplicadas y en Sistemas, Universidad Nacional Autónoma de México, Apartado Postal 20-726, Delegación de Álvaro Obregón, 01000 México, DF., México

ARTICLE INFO

Article history:
Received 28 August 2009
Received in revised form
27 November 2010
Accepted 29 November 2010
Available online 13 December 2010

Keywords:
Effective properties
Imperfect contact
Periodic composites
Asymptotic homogenization

ABSTRACT

In this contribution, effective elastic moduli are obtained by means of the asymptotic homogenization method (AHM), for oblique two-phase fibrous periodic composites with two models (*spring* and *interphase*) of imperfect contact conditions. This work is an extension of previous reported results, where only perfect contact for elastic or piezoelectric composites for square and hexagonal arrays were considered. The constituents of the composites exhibit transversely isotropic properties. A doubly periodic parallelogram array of cylindrical inclusions under longitudinal shear is considered. The behavior of the shear elastic coefficient for different geometry arrays related to the angle of the cell is studied. As validation of the present method, some numerical examples and comparisons with theoretical and experimental results verified that the present model is efficient for the analysis of composites with presence of imperfect interface and parallelogram cell. The effect of the arrangement of the cells on the shear effective property is observed. The present method can provide benchmark results for other numerical and approximate methods.

1. Introduction

The transport properties of circular cylinders packed in regular arrays are of considerable interest in a number of fields. The transport property may be the electrical or thermal conductivities, the dielectric permittivity, or the elastic shear modulus in antiplane elasticity. The result is of interest in the field of materials physics where two phase materials containing rod- or fiber-like inclusions often occur. Knowledge of their electrical or thermal conductivities and their elastic properties is valuable. Calculations on ordered arrays of cylinders are therefore directly relevant to practical situations. The problem of calculating the transport properties will be discussed here in the context of stiffness elastic properties. However, the mathematics and the results obtained are immediately applicable to other associated situations.

In most composites, the fiber–matrix adhesion is imperfect; the continuity conditions for stresses and displacements are not satisfied. Thus various approaches have been used, in which the bond between the reinforcement and the matrix is modeled by an interphase with specified thickness, by Hashin [1], Guinovart-Diaz et al. [2]. Other assumptions suppose that the contrast or jump of the displacements in the interface is proportional to the corresponding component of the tension in the interface in terms of a parameter given by the constant of a spring. This type of imperfect contact (*spring type*) in the interphases of the composites was investigated by Benveniste and Miloh [3] among others and has been used later, for instance, by Achenbach and Zhu [4] and Hashin [5–7].

Molkov and Pobedria [8] reported the elastic effective coefficients for two-phase fibrous composite with rhombic array of periodic cells under perfect contact conditions. Recently, Abolfathi [9] applied a numerical algorithm to determine the homogenized elastic properties of bidirectional fibrous composites and Jiang et al. [10] analyzed different situations of parallelogram composite. In this work, micromechanical analysis method is applied to a periodic composite with unidirectional fibers and parallelogram cells, in particular, rhombic periodic cells. The analytical expressions of the homogenized elastic properties are calculated for two phase composite with imperfect contact conditions. Two approaches (spring and three phase models) are used for the calculation of the shear elastic effective coefficients of angular fibrous composites with anisotropic elastic constituents with no well bonded contact. This contribution is an extension of previous works of Rodriguez-Ramos et al. [11] and Guinovart-Diaz et al. [12] using the asymptotic homogenization method (AHM). The results in this paper are mainly focused on the impact of the fibers cross angles

* Corresponding author. Tel.: +53 7 832 2466.
E-mail addresses: jclrealpozo@matcom.uh.cu (J.C. López-Realpozo), reinaldo@matcom.uh.cu, rerora2006@gmail.com (R. Rodríguez-Ramos), guino@matcom.uh.cu (R. Guinovart-Díaz), jbravo@matcom.uh.cu (J. Bravo-Castillero), fjs@mym.iimas.unam.mx (F.J. Sabina).

0020-7403/$ - see front matter © 2010 Elsevier Ltd. All rights reserved.
doi:10.1016/j.ijmecsci.2010.11.006

and the mechanical imperfection of the interface on the stiffness properties of the chosen composites.

2. General considerations. Contact at the interfaces

Let us consider unidirectional periodic fibers composite with crossing angle θ embedded in a matrix as shown in Fig. 1. The crossing angle of the fibers is assumed to remain constant so that a parallelogram cell with periods w_1, w_2 can be defined. The periodicity of microstructure determines the geometry of the periodic cell S. Thus, a two-phase periodic composite is considered here which consists of a parallelogram array of identical parallel circular cylinders embedded in a homogeneous medium (Fig. 2). As a unidirectional fibrous composite it is assumed that the microstructure of the composite along the third direction (perpendicular to plane of cross-section) remains constant. The fibers are all assumed straight and of circular cross sections with radius R. The material properties of each phase belong to the crystal symmetry class 6 mm, where the axes of material and geometric symmetry are parallel. The composite is not well bonded at the contact between the matrix and the fiber. Therefore, imperfect contact conditions at the interface Γ are considered.

The governing elastic equations for this kind of materials are the Navier equations of linear elasticity. As the body forces are absent, stress ($\boldsymbol{\sigma}$), strain ($\boldsymbol{\varepsilon}$), and displacement ($\boldsymbol{u}=(u_1, u_2, u_3)$) fields satisfy the following three equations, respectively:

$$\text{Stress–strain relations: } \boldsymbol{\sigma} = \mathbf{C}:\boldsymbol{\varepsilon}. \tag{1}$$

$$\text{Displacement-strain relations : } \boldsymbol{\varepsilon} = \frac{1}{2}(\nabla\mathbf{u} + \nabla^{\mathrm{T}}\mathbf{u}). \tag{2}$$

$$\text{Equilibrium equations : } \nabla\cdot\boldsymbol{\sigma} = 0, \tag{3}$$

where $\mathbf{C}$ is the elasticity tensor and ∇ is the gradient operator, comma notation is understood to denote differentiation with respect to x_i.

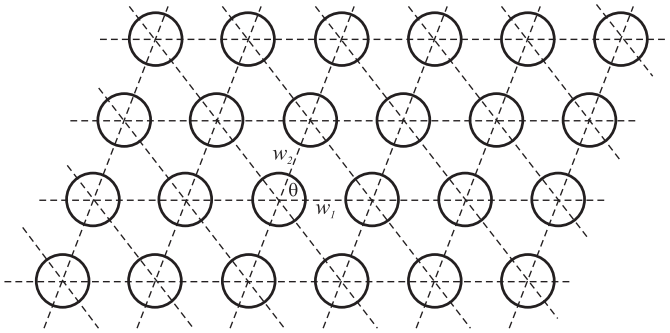

Fig. 1. The cross-section of a rhombic array of angle θ and periods w_1, w_2 of circular fibers.

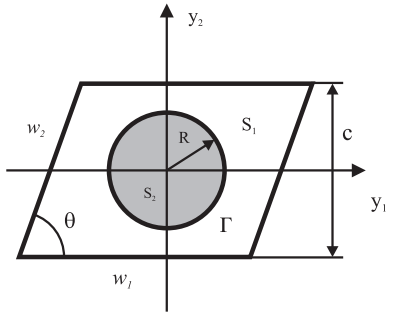

Fig. 2. The unit cell showing the domains S_1 and S_2 occupied by the matrix and fibers materials; Γ is the common interface.

Since most reinforcements may not be perfectly bonded to their surrounding matrix, the perfect bonding condition is often inadequate in describing the physical and mechanical behavior of real composite materials. An imperfect bond may be introduced deliberately by coating the reinforcements to control the properties of the composites and sometimes to improve their fatigue life [1]. Moreover, chemical reactions between reinforcements and the matrix in manufacturing process or the damage caused by cyclic loadings of the composites can develop imperfect bonding interfaces. To model the imperfect bonding at the interfaces, some idealized interfacial conditions have been proposed by various investigators. For example, Gharemani [13], Mura and Furuhashi [14], Mura et al. [15], and Jasiuk et al. [16], among others have used the pure frictionless sliding condition to model grain boundary sliding in polycrystalline materials and particle sliding in soil. Furthermore, the frictional sliding considered by numerous researchers; see, for example, Hashin [1,5], Jasiuk et al. [17], Huang et al. [18], Gao [19], and Zhong and Meguid [20] is a more realistic interfacial condition, in which the frictional resistance of the interface is accommodated by assuming that the discontinuous components of displacement are proportional to the associated tractions

$$\begin{aligned} &\|\sigma_{ij}\| n_j = 0, \\ &\|u_l\|(\delta_{il} - n_i n_l) = (1/K)T_i, \quad \text{on } \Gamma \\ &\|u_l\| n_i n_l = (1/M)N_i \end{aligned} \tag{4}$$

where $T_i = \sigma_{ij}n_j - \sigma_{lm}n_l n_m n_i$ and $N_i = \sigma_{lm}n_l n_m n_i$ are the shear and normal components of the surface traction, respectively. Γ denotes the interface between the fibers and matrix, whereas K and M are values of sliding and debonding parameters. As these parameters become infinite, the perfect bonding condition is recovered, while pure sliding condition occurs when K is zero and M approaches infinity. Since these parameters are related to the macroscopic behavior of composites, the theory suggests that they can be determined by a set of carefully designed experiments.

Since a binary periodic composite is studied, thus, two distinct phases, occupying S_1 and S_2 (Fig. 2) are assumed to be in non-perfect contact along the interface Γ of each cylinder. In order to model various possible damages occurring on the fiber-matrix interface composite two formulations of imperfect bonded are considered as follows:

(i) *Linear spring interface (LSI) model.* A generalized shear lag model [1,5] that can be termed as the mechanically compliant weakly conducting interface is useful for the analysis of the behavior of composites. The imperfect interface proposed is the shear lag model (or the spring layer model): tractions are continuous but displacements are discontinuous across the imperfect interface. The jumps in displacement components are further assumed to be proportional, in terms of the "spring-factor-type" interface parameter, to their respective interface traction components

$$\sigma_t^{(\alpha)} = \widehat{K}\|u_t\|, \quad \overleftrightarrow{\sigma}^{(1)}\cdot\vec{n}^{(1)} = \overleftrightarrow{\sigma}^{(2)}\cdot\vec{n}^{(2)}, \quad u_n^{(1)} = u_n^{(2)}, \text{ on } \Gamma \tag{5}$$

where the subscripts t and n means tangential and normal directions respectively. $\widehat{K}$ is the proportional interface parameter. The double bar notation is used to denote the jump of the relevant function across the interphase Γ taken from the matrix (1) to the fiber (2) i.e. $\|f\| = f_1 - f_2$. Eq. (5) is usually called a weak interface condition. It has been originally proposed by Goland and Reissner [21], later studied by many authors like Benveniste and Miloh [3], Molkov and Pobedria [22], Mahiou and Beakou [23], and Andrianov et al. [24].

(ii) *Interphase contact (IC) model.* The imperfect interface condition is replaced by the explicit three-phase problem of two

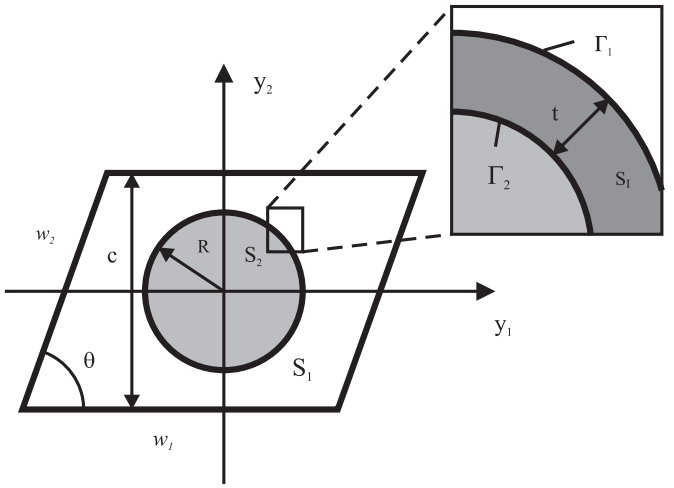

Fig. 3. Parallelogram periodic cell of composite, with a thickness interphase t of another material between the matrix and fiber. Here Γ_1 and Γ_2 denote the common interfaces between matrix and interphase, and interphase and fiber, respectively.

constituents and an interphase of certain thickness (t), with two perfect interfaces conditions at Γ_1 and Γ_2 (Fig. 3). The region occupied by the matrix, the fiber and the interphase in the periodic cell are denoted by S_1, S_2 and S_I, respectively. The common region between the matrix S_1 and the interphase S_I is a circumference of radio $R+t$, denoted by Γ_1 where t is the thickness of interphase. The common region between the interphase S_I and the fiber S_2 is a circumference of radio R denoted by Γ_2 (see in Fig. 3 the corresponding periodic cell).

Linear spring interface and interphase contact conditions, in this article, referred to as imperfect bonding, is rather more general in the sense that the pure sliding and perfect interface can be achieved as its special cases. The most general form of the constitutive relation for interfacial conditions can be obtained from interatomic potentials [25, 26]. Based on nonlinear Needleman-type interfaces, Levy and Dong [27] and Levy [28–29] obtained the effective response of fiber composites subjected to transverse shear, axial tension, and antiplane shear. Besides having a number of phenomenological fit parameters, which are not easy to be determined, the problems with nonlinear interfacial conditions are usually very complicated. This work is based on expanding the capability of the theoretical models available in the literature to get closer to realistic composites. Bonding between phases is a point that requires attention. In that sense, we are presenting a contribution using the linear spring model as possible mathematical description of imperfections in the composites although its limitation for effects of debonding or partial debonding which very often occurs. Discussions on nonlinear interface models by asymptotic homogenization method are open points for further research.

In the forthcoming sections some summary ideas of the antiplane problem and a brief comment about asymptotic homogenization method (AHM) are given. The statement of the local problems for both formulations (i) and (ii) are written and the corresponding solutions are found. The effective coefficients are calculated for both models of imperfect contacts. Analysis of the results is discussed.

3. Asymptotic homogenization method (AHM) and antiplane problems

In a two-dimensional situation, like in the considered geometry here, it turns out that the above equations uncouple into two independent systems under suitable boundary conditions. Just like, the familiar plane- and anti-plane-strain deformation states in linear elasticity see Pobedria [30] and Camacho-Montes et al. [31]. One of them involves u_1, u_2, i.e., it is a state of in-plane mechanical deformation fields. The other state, which is of particular interest in this work, is characterized by an out-of-plane mechanical displacement u_3 which is a function of the plane global variables x_1 and x_2. The main aim of this paper is the determination of effective properties in two-phase composites for the out-of-plane using the homogenization method, say, as in Camacho-Montes et al. [31] and Lopez-López et al. [32], but now considering mechanical imperfect conditions at the interfaces. In this case the relevant constitutive relations (1) and (2) are

$$\sigma_{13} = 2C_{1313}\varepsilon_{13}, \tag{6}$$

$$\sigma_{23} = 2C_{2323}\varepsilon_{23}, \tag{7}$$

where σ_{13}, σ_{23} are the components of out-of-plane mechanical stress, C_{1313} and C_{2323} are the elastic modulus and the differential $2\varepsilon_{13}=u_{3,1}$, $2\varepsilon_{23}=u_{3,2}$ denote the components of the mechanical strain. The equilibrium equations (3) are transformed into

$$\left(C_{3\alpha 3\beta}(\mathbf{y})u_{3,\beta}\right)_{,\alpha} = 0, \tag{8}$$

where the Greek indices run from 1 to 2, and $\mathbf{y}=\mathbf{x}/\varepsilon$ is the local variable with $\varepsilon=l/L$ is a small geometrical parameter relating the distance l between the centers of two neighboring cylinders and the diameter L of the composite.

Eq. (8) has S-periodic coefficients and they are rapidly oscillating (see, Fig. 1). In order to obtain the homogenized equation and the corresponding effective coefficients, the solution of Eq. (8) is sought using the method of two scales by the ansatz

$$u_3(\mathbf{x}) = v_0(\mathbf{x}) + \varepsilon v_1(\mathbf{x},\mathbf{y}) + O(\varepsilon^2), \tag{9}$$

being v_1 is a S-periodic function respect to y. Substituting Eq. (9) into Eq. (8), applying the chain rule considering that $\mathbf{x}$ and $\mathbf{y}$ are independents, and equating the terms of orders ε^{-1}, ε^0 to zero, one can obtain that $v_1(\mathbf{x},\mathbf{y}) = {}_{\alpha 3}N(\mathbf{y})v_{0,\alpha}(\mathbf{x})$ where $v_0(\mathbf{x})$ is solution of the homogenized equation $C^*_{3\alpha 3\beta}v_{0,\alpha\beta}=0$, where $C^*_{3\alpha 3\beta} = \left\langle C_{3\alpha 3\beta}(\mathbf{y}) + C_{3\alpha 3\delta}(\mathbf{y})\,{}_{\alpha 3}N_{,\delta}(\mathbf{y})\right\rangle$ are the so-called effective coefficients. The comma will be also used to denote derivative respect to the local variable. The angular brackets define the volume average per unit length over the unit cell, that is, $\langle F\rangle = \int_S F(y)dy$.

The computation of effective coefficients depends on the solution of problems over the periodic cell in order to obtain the local functions ${}_{\alpha 3}N(\mathbf{y})$. The solution of such local problems (called in the sequel as ${}_{\alpha 3}L$), on the periodic cell described in Fig. 2, taking into account the imperfect contact conditions (5) is one of the main objectives of the present work. It is a well-known derivation whose details can be found elsewhere and here is omitted (see, for instance, [30, 33]).

Of a greater interest are the so-called local (or canonical) problems associated here with the correction term v_1 to the mean variations v_0, since they appear in the formulae of the effective properties. There are two of such problems, which are referred as ${}_{13}L$ and ${}_{23}L$. A pre-index is used to distinguish the functions such as displacements for different local problems, which appear below.

Due to the linearity of Eqs. (5)–(8), the correction term v_1, can be obtained as a linear combination of some of such displacements and potentials. This, however, will not be done here, since the main objective of this paper is the characterization of the three effective properties $p_{11}=C^*_{1313}$, $p_{12}=C^*_{1323}$, $p_{21}=C^*_{2313}$ and $p_{22}=C^*_{2323}$. The symmetries of composite and constitutive materials lead us to find one alternative form to obtain p_{11} and p_{22} and two alternatives for obtaining $p_{12}=p_{21}$ properties as follows:

$$p_{11} = p_1V_1 + p_2V_2 + \langle p_{13}N_{,1}\rangle, \tag{10}$$

$$p_{12}=p_{21}=\langle p_{13}N_{,2}\rangle=\langle p_{23}N_{,1}\rangle, \tag{11}$$

$$p_{22}=p_1V_1+p_2V_2+\langle p_{23}N_{,2}\rangle, \tag{12}$$

where $p_\gamma=C^{(\gamma)}_{1313}$ with $\gamma=1, 2$ denotes the shear moduli of matrix and fibers, respectively; ${}_{13}N$ and ${}_{23}N$ are functions of $z=y_1+iy_2$ [31] that are solutions of the local problems ${}_{13}L$ and ${}_{23}L$, respectively. $V_2=\pi R^2/V$ and $V_1=1-V_2$ are the percentages of concentrations of matrix and fiber respectively, and $V=|w_1||w_2|\sin\theta$ is the area of periodic cell.

4. The antiplane (spring) problems ${}_{\alpha 3}L$

The mathematical statement of the problem consists to find doubly periodic functions ${}_{\alpha 3}N={}_{\alpha 3}N^{(\gamma)}(\mathbf{y})$ if $\mathbf{y}\in S_\gamma$, which satisfy the following Laplace equation with the conditions:

$$\nabla^2{}_{\alpha 3}N^{(\gamma)}=0, \quad \text{in} \quad S_\gamma, \tag{13}$$

$$p_\gamma({}_{\alpha 3}N^{(\gamma)}_{,1}n_1+{}_{\alpha 3}N^{(\gamma)}_{,2}n_2)+p_\gamma n_\alpha=\widehat{K}\|{}_{\alpha 3}N^{(\gamma)}\|, \quad \text{on} \quad \Gamma, \tag{14}$$

$$\|p_\gamma({}_{\alpha 3}N^{(\gamma)}_{,1}n_1+{}_{\alpha 3}N^{(\gamma)}_{,2}n_2)\|=-\|p_\gamma\|n_\alpha, \quad \text{on} \quad \Gamma, \tag{15}$$

$$\langle {}_{\alpha 3}N\rangle=0, \quad \text{in} \quad S=S_1\cup S_2, \tag{16}$$

the outward unit normal vector to the interface Γ is $\mathbf{n}=(n_1,n_2)$. The pre-index used in Eqs. (13)–(16) for the local function will be omitted for simplicity. The problem (13)–(16) should be converted into dimensionless problems making the appropriate change. Defining the dimensionless variable $\xi=y/l$ (this is not a small parameter!), then $N^{(\gamma)}_{,i}=u^{(\gamma)}{}_{,i}$ and $N^{(\gamma)}_{,ii}=u^{(\gamma)}_{,ii}/l$ where $u^{(\gamma)}=N^{(\gamma)}/l$ and the derivative $u_{,i}$ is with respect to the variable ξ_i. The interface parameter is replaced by $\widehat{K}=Kp_1/R_o$, K is a dimensionless parameter and R_0 is the true radius of the fibers in the composite. Also the dimensionless parameter $R=R_o/l$ is introduced. The dimensionless problem related to Eqs. (13)–(16) over the periodic cell Y are now rewritten below

$$\nabla^2u^{(\gamma)}=0, \quad \text{in} \quad S_\gamma, \tag{17}$$

$$\frac{p_\gamma(u^{(\gamma)}_{,1}n_1+u^{(\gamma)}_{,2}n_2)+p_\gamma n_\alpha}{p_1}=\frac{K}{R}\|u^{(\gamma)}\|, \quad \text{on} \quad \Gamma, \tag{18}$$

$$\left\|\frac{p_\gamma(u^{(\gamma)}_{,1}n_1+u^{(\gamma)}_{,2}n_2)}{p_1}\right\|=-(1-\kappa)n_\alpha, \quad \text{on} \quad \Gamma, \tag{19}$$

$$\langle u\rangle=0, \ \text{in} \ S=S_1\cup S_2, \tag{20}$$

where $\kappa=p_2/p_1$ and $u=u^{(\gamma)}$ if $\xi\in S_\gamma$.

5. Solution of local (imperfect spring) problems ${}_{\alpha 3}L$ ($\alpha=1,2$)

The well-developed theory of analytical functions in [34] can be applied to solve the problem (17)–(20). Doubly periodic harmonic functions are to be found for the ${}_{\alpha 3}L$ local problems in terms of the following expansions of harmonic functions:

$$u^{(\gamma)}=\mathrm{Re}\{\varphi_\gamma(z)\}, \tag{21}$$

where

$$\varphi_1=\frac{a_oz}{R}+\sum_{k=1}^{\infty}{}^o\left(\frac{\zeta^{(k-1)}(z/R)}{(k-1)!}\right)a_k \text{ and } \varphi_2(z)=\sum_{p=1}^{\infty}{}^o\left(\frac{z}{R}\right)b_p, \tag{22}$$

$\zeta(z)$ is the Weierstrass' ζ quasi-periodic function defined as

$$\zeta(z)=\frac{1}{z}+\sum_{m,n}{}'\left(\frac{1}{z-P_{nm}}+\frac{1}{P_{nm}}+\frac{z}{P^2_{nm}}\right),$$

$P_{nm}=nw_1+mw_2$, for $m, n\in Z$, and the prime over the summation symbol means that the pair $(m, n)=(0, 0)$ is excluded. Laurent's expansion of function $\varphi_1(z)$ is given by the following expression:

$$\varphi_1(z)=\frac{z}{R}a_0+\sum_{p=1}^{\infty}{}^o\left(\frac{R}{z}\right)a_p-\sum_{p=1}^{\infty}{}^o\sum_{k=1}^{\infty}{}^o\left(\frac{z}{R}\right)\sqrt{\frac{k}{p}}w_{kp}a_k, \tag{23}$$

where

$$w_{kp}=\frac{(k+p-1)!}{(k-1)!(p-1)!}$$

$$\frac{S_{k+p}R^{k+p}}{\sqrt{k\sqrt{p}}}, \ S_{k+p}=\sum_{m,n}(mw_1+nw_2)^{-(k+p)}, \ m^2+n^2\neq 0, \ k+p\geq 2, \ S_2=0.$$

The constants a_o, a_p, b_p and $z=\xi_1+i\xi_2$ are complex numbers; the over bar indicate complex conjugate and the superscript "o" on the summation indicates that the sum is carried out only over odd indices, w_1, w_2 are the periods.

From the condition of double periodicity of the function u follows $a_o=\chi R^2H_1\overline{a}_1+\chi R^2H_2a_1$, where

$$H_1=\frac{\overline{\delta}_1\overline{w}_2-\overline{\delta}_2\overline{w}_1}{w_1\overline{w}_2-w_2\overline{w}_1}, \quad H_2=\frac{\delta_1\overline{w}_2-\delta_2\overline{w}_1}{w_1\overline{w}_2-w_2\overline{w}_1},$$

with $\delta_i=\zeta(z+w_i)-\zeta(z)$, and after some algebraic manipulations, the following system of equations is obtained in order to find the complex unknown coefficients a_k by the system

$$\overline{a}_p+\beta_1R^2H_1\overline{a}_1\delta_{1p}+\beta_1R^2H_2a_1\delta_{1p}+\beta_p\sum_{k=1}^{\infty}{}^ow_{kp}a_k=R\beta_1\delta_{1p}(\delta_{1\alpha}-i\delta_{2\alpha}), \tag{24}$$

where δ_{kp} is Kronecker's delta and

$$\beta_p=\frac{(1-\kappa)K+p\kappa}{(1+\kappa)K+p\kappa}$$

In order to find the solution of the system (24), it is reduced into two subsystems with real and imaginary separated parts. The magnitudes $a_k=x_k+iy_k$, $H_\gamma=h_{1\gamma}+ih_{2\gamma}$, $w_{kp}=w_{1kp}+iw_{2kp}$ where x_k, y_k, $h_{1\gamma}$, $h_{2\gamma}$, w_{1kp} and w_{2kp} are real numbers, represent the real or imaginary parts of complex numbers a_k, β_pH_1, H_2, w_{kp}, respectively.

The system (24) for $p=1$ is written in compact form as follows:

$$(I+\beta_1R^2J)X+\beta_1N_1X_1=R_1\beta_1B, \tag{25}$$

where I represents the 2×2-unit matrix, J is the square matrix defined by

$$J=\begin{pmatrix}(h_{11}+h_{12}) & (h_{21}-h_{22})\\ (-h_{21}-h_{22}) & (h_{11}-h_{12})\end{pmatrix},$$

the infinite matrix $N_1(n_{k1})$ is composed by two rows or horizontal square blocks of order 2 of the form

$$n_{k1}=\begin{pmatrix}w_{1k1} & -w_{2k1}\\ -w_{2k1} & -w_{1k1}\end{pmatrix}, \ k=2s+1.$$

Moreover, the transpose vectors of unknowns $X_1^T=(x_1,y_1)$, $B^T=(\delta_{1\alpha}, \delta_{2\alpha})$ and $X^T=(x_3, y_3,\ldots,x_k, y_k,\ldots)$ are given.

The system (24) for $p\geq 3$ are transformed into

$$(I+W)X_2=-N_2X_1, \tag{26}$$

where the matrix $W=W(n_{kp})$ is composed by square blocks of order 2 of the form

$$n_{kp}=\chi_p\begin{pmatrix}w_{1kp} & -w_{2kp}\\ -w_{2kp} & -w_{1kp}\end{pmatrix},$$

$k=2s+1$, $p=2t+1$, $s=t=1,2,3,\ldots$ and $N_2=N_2(n_{1p})$ is formed by two columns or vertical square blocks of order 2. From (26) follows

$X_2=-(I+W)^{-1}N_2X_1$ and substituting into (25) results

$$a_1=(1,i)R\left(I+\beta_1R^2J-\beta_1N_1(I+W)^{-1}N_2\right)^{-1}B. \tag{27}$$

In order to determine the effective properties it is necessary to truncate the system of equations (24) in an appropriate order $k=p=N_0$. A very important first approximation is obtained if we consider $N_0=1$, in this case only survives the unknowns with subscripts $k=1$ for the system (24). It is easy to solve this system and its solution is

$$\begin{pmatrix}x_1\\ y_1\end{pmatrix}=R(I+\beta_1R^2J)^{-1}B. \tag{28}$$

Introducing the notation

$$Z=I+\beta_1R^2J-\beta_1N_1(I+W)^{-1}N_2, \tag{29}$$

the following explicit expressions of a_1 are obtained from Eq. (27) for the local problems ${}_{13}L$ and ${}_{23}L$, respectively

$$a_1=R\beta_1(z_{22}-iz_{21})/|Z|, \tag{30}$$

$$a_1=-(R\beta_1(z_{12}-iz_{11}))/|Z|, \tag{31}$$

where $|Z|$denotes the determinant of numerical symmetric matrix Z.

6. Effective properties (imperfect spring)

Eqs. (10)–(12) are easily transformed applying Green's theorem to the area integrals. Replacing $N^{(\gamma)}=u^{(\gamma)}/l$, $dy_i=ld\xi_i$ the effective coefficients p_{11}, p_{12}, p_{21} and p_{22} are connected by the following relations:

$$p_{11}-ip_{21}=p_1V_1+p_2V_2-\frac{p_1}{V}\left(i\int_\Gamma u^{(1)}d\xi_1+\int_\Gamma u^{(1)}d\xi_2\right)+\frac{p_2}{V}\left(i\int_\Gamma u^{(2)}d\xi_1+\int_\Gamma u^{(2)}d\xi_2\right), \tag{32}$$

$$p_{12}-ip_{22}=-i(p_2V_1+p_2V)-\frac{p_1}{V}\left(i\int_\Gamma u^{(1)}d\xi_1+\int_\Gamma u^{(1)}d\xi_2\right)+\frac{p_2}{V}\left(i\int_\Gamma u^{(2)}d\xi_1+\int_\Gamma u^{(2)}d\xi_2\right), \tag{33}$$

where V_1 and $V_2=\pi R^2/V$ are the volume fraction of matrix and inclusion, respectively, $V_1+V_2=1$ and $V=|w_1||w_2|\sin\theta$ denotes the volume of the parallelogram periodic cell. In Eq. (32) $u^{(\gamma)}$ is the solution of the local problem ${}_{13}L$ whereas in Eq. (33) $u^{(\gamma)}$ is the solution of the ${}_{23}L$. Taking into account (21)–(23) and the orthogonality of the system of functions $\{e^{inx}\}_{n=-\infty}^{\infty}$ in $[0,2\pi]$, simple analytical formulae for effective properties are deduced from Eqs. (32) and (33) depending only on the unknown a_1 as follows:

$$p_{11}-ip_{12}=p_1(1-2V_2\bar{a}_1/R), \tag{34}$$

$$p_{21}-ip_{22}=-p_1(i+2V_2\bar{a}_1/R), \tag{35}$$

where a_1 in Eqs. (34) and (35) are given by Eqs. (30) and (31), respectively. Finally, the effective coefficients can be written as

$$p_{11}=p_1(1-2V_2\beta_1z_{22}/|Z|), \tag{36}$$

$$p_{12}=2p_1V_2\beta_1z_{21}/|Z|, \tag{37}$$

$$p_{21}=2p_1V_2\beta_1z_{12}/|Z|, \tag{38}$$

$$p_{22}=p_1(1-2V_2\beta_1z_{11}/|Z|). \tag{39}$$

The analytical expressions of effective properties (36)–(39) are functions of the properties and volume fractions of constituents, of periodic cell w_1, w_2 and the imperfect parameter K. The effective properties of a composite with perfect adhesion between the constituents are obtained from Eqs. (36)–(39) taking $K\to\infty$ and the total separation occurs when $K\to0$. From the symmetric matrix Z is deduced $p_{12}=p_{21}$. The effective coefficients p_{11}, p_{22} and $p_{12}=p_{21}$ represent the effective axial coefficients of an orthotropic fiber reinforced composite with defect at the interface Γ.

7. Local (three phase) problems ${}_{\alpha3}L$ and effective properties

The statement and the solution of the local problems as well as the effective coefficients for three phase models are calculated in analogous way to the spring interface model reported in previous sections. Therefore, in this section we shall not repeat the same procedure and only some fundamental ideas will be explained and the closed form expressions of the effective coefficients will be written.

The dimensionless antiplane local problems for three-phase composite [12] over periodic cell $S=S_1\cup S_I\cup S_2$ (Fig. 2) are written below

$$\nabla^2u^{(\tau)}=0,\quad \text{in}\quad S_\tau(\tau=1,2,I) \tag{40}$$

$$\|u^{(\gamma)}\|=0,\quad \text{on}\quad \Gamma_\gamma,\quad \gamma=1,2 \tag{41}$$

$$\left\|\frac{p_\gamma(u_{,1}^{(\gamma)}n_1+u_{,2}^{(\gamma)}n_2)}{p_1}\right\|=-(1-\kappa_\gamma)n_\alpha,\quad \text{on}\quad \Gamma_\gamma, \tag{42}$$

$$\langle u\rangle=0,\ \text{in}\ S\ \text{and}\ u=u^{(\tau)}\quad \text{if}\ \xi\in S_\tau \tag{43}$$

where the subscript I denotes the interphase properties , $\kappa_1=p_I/p_1$ and $\kappa_2=p_2/p_1$, $||f^{(1)}||=f_1-f_I$ and $||f^{(2)}||=f_I-f_2$. From the conditions (41) and (42) the continuity of displacements and tractions on the interfaces Γ_1 and Γ_2 are derived, respectively.

The solution of the problems (40)–(42) are sought analogous to the problems (17)–(19) and the axial effective coefficients for three phase are calculated in the same manner, thus we have

$$p_{11}=p_v-p_1(V_I+V_2)F\frac{((\chi_1+1)z_{22}-|Z|)}{\chi_1|Z|}-G(\kappa_1-\kappa_2)^2V_IV_2, \tag{44}$$

$$p_{12}=p_1(V_I+V_2)F\frac{(\chi_1+1)z_{21}}{\chi_1|Z|}, \tag{45}$$

$$p_{21}=p_1(V_I+V_2)F\frac{(\chi_1+1)z_{12}}{\chi_1|Z|}, \tag{46}$$

$$p_{22}=p_v-p_1(V_I+V_2)F\frac{((\chi_1+1)z_{11}-|Z|)}{\chi_1|Z|}-G(\kappa_1-\kappa_2)^2V_IV_2, \tag{47}$$

where p_v refers to the Voigt average of material constants, $p_v=p_1V_1+p_IV_I+p_2V_2$, $V_2=\pi R^2/V$ is the volume fraction of fiber, V_I is the volume fraction of the interphase S_I, $V_1=1-V_I-V_2$ is the volume fraction of the matrix. The numerical matrix Z with components z_{ij} is given in Eq. (29) replacing β_p by χ_p and

$$\chi_p=\frac{(1-\kappa_1)(\kappa_1+\kappa_2)(V_I+V_2)^p+(1+\kappa_1)(\kappa_1-\kappa_2)V_3^p}{(1+\kappa_1)(\kappa_1+\kappa_2)(V_I+V_2)^p+(1-\kappa_1)(\kappa_1-\kappa_2)V_3^p},$$

$$F=E\left[\frac{V_I(\kappa_1+\kappa_2)(1-\kappa_1)+2V_2\kappa_1(1-\kappa_2)}{(V_I(\kappa_1+\kappa_2)+2V_2\kappa_1)}\right],$$

$$E=\frac{(V_I(\kappa_1+\kappa_2)(1-\kappa_1)+2V_2\kappa_1(1-\kappa_2))}{V_I(\kappa_1+\kappa_2)(1+\kappa_1)+2V_2\kappa_1(1+\kappa_2)},$$

$$G=\frac{1}{(V_I(\kappa_1+\kappa_2)+2V_2\kappa_1)}.$$

The coefficients (44)–(47) represent the effective axial coefficients of an orthotropic fiber reinforced composite with interphase S_I. The analytical expressions of effective properties (44)–(47) are

functions of the properties and volume fractions of constituents, of periodic cell w_1, w_2. The two-phase composite with perfect contact on interface Γ reported in Guinovart et al. [12] is obtained from Eqs. (44)–(47) taking the parameter $\kappa_1 = p_I/p_1 \to \infty$ or $V_I = 0$. The complete separation is obtained when $\kappa_1 = p_I/p_1 \to 0$.

In the case as the area of annulus S_I is very thin, very good coincidence exists between the imperfect spring (36)–(39) and three-phase models (44)–(47). A condition between the interface and interphase parameters is found. Thereby, the volume fraction of interphase is $V_I = \pi(t^2 + 2tR)/V$ where t is the thickness of layer S_I (see Fig. 3) and the relationship between the non-dimensional debonding parameter K and the interphase property κ_1 can be introduced as in Ref. [1], in the following form:

$$K = R\kappa_1/t. \tag{48}$$

8. Analysis of the results

In order to illustrate the broad applicability of the theory developed above several examples are chosen.

(1) Let us consider the unit cell shown in Fig. 2. A parallelogram of vertex angle θ and periods $w_1 = 1$, $w_2 = e^{i\theta}$. Two special cases of rhombic array, where $\theta = 90^\circ$ for a square array and $\theta = 60^\circ$ for a hexagonal array were studied in Rodriguez-Ramos et al. [35] and Guinovart-Diaz et al. [36] for perfect contact conditions. In these two special cases, the composite material is transversely isotropic. However, the global behavior of the composite is orthotropic in more general array of cells, different from $\theta = 60^\circ$ and $\theta = 90^\circ$ (see [11, 12]). First we modeled LSI and computed p_{11}/p_1, p_{12}/p_1 and p_{22}/p_1 vs. V_2 for $\theta = 30^\circ$, $\theta = 45^\circ$, $\theta = 75^\circ$ and three values of the imperfection parameter, which correspond to debonding alone the interface, $K = 10^{-5}$, and imperfect spring interface, $K = 10$, and perfect contact between matrix and fiber, $K = 10^{10}$. The matrix and fiber shear moduli are isotropic and are taken such that $\kappa = p_2/p_1 = 120$. Latter already analyzed in Rodriguez-Ramos et al. [11] and Guinovart-Diaz et al. [12] helps us to compare the results. Ours reproduce those of Refs. [11–12]. The dimensionless effective shear moduli against fiber volume fraction are displayed in Table 1. Note that the imperfection parameter $K = 10$ always degrades the effective properties. A 19% reduction, for instance, is noted for p_{22}/p_1 at $V_2 = 0.4$, $\theta = 45^\circ$.

(2) The effect of elastic interface imperfection on shear dimensionless effective coefficients p_{22}/p_1, p_{11}/p_1 and p_{12}/p_1 for an anisotropic composite made of T300 fibers embedded in an epoxy matrix is shown in Figs. 4–6, for no principal axis. The material parameters are taken from Hashin [5]. The effective properties are calculated by the two AHM imperfect contact approaches (36)–(39) (red discontinuous line) and three-phase models (44)–(47) (yellow circles), considering a rhombic periodic cell with $\theta = 30^\circ$ and three different volume fiber fraction $V_2 = 0.4$ (square), $V_2 = 0.3$ (triangle) and $V_2 = 0.2$ (star). The comparisons illustrate that the two models are coincident, where the relationship (48) for imperfect parameter is used in the computation. The anisotropic character of this composite can be observed in Figs. 4–5 where the values of the coefficient for p_{22}/p_1 reach higher values than the one obtained for p_{11}/p_1, mainly for perfect contact $K \to \infty$. The more pronounced effective properties are obtained for the higher volume fraction for $K > 1$, the opposite situation is obtained for $K < 1$ because of the total disjoint between the matrix and fibers. If $K = 1$, the properties are almost independent of the volume fraction. Another remark is related to the rapid increasing of the properties when the imperfect parameter K is in the neighborhood of 1. For other cases, the overall properties are constant. This situation is the same as that shown in Hashin [5] (in Fig. 6) for isotropic composite and hexagonal symmetry ($\theta = 60^\circ$).

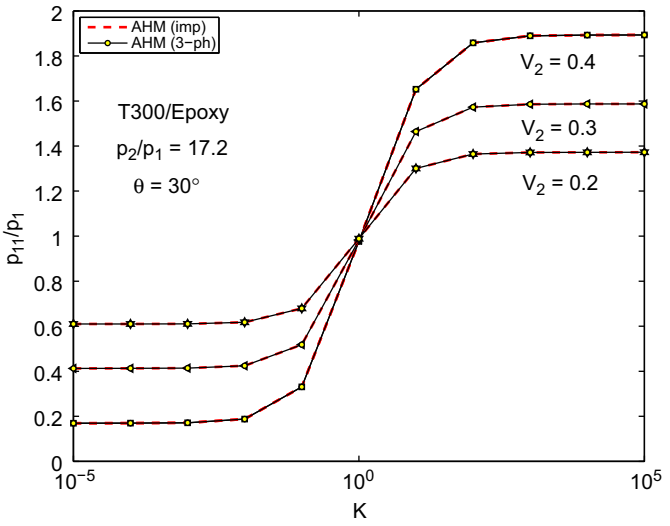

Fig. 4. The effect of elastic interface imperfection on shear dimensionless effective coefficient p_{22}/p_1, for an anisotropic composite T300 fibers and epoxy matrix for different fiber volume fraction.

Table 1
Effective elastic moduli p_{11}/p_1, p_{12}/p_1 and p_{22}/p_1 of a rhombic array and fiber debonding $K = 10^{-5}$, imperfect contact $K = 10$ and perfect contact $K = 10^{10}$, for three different periodic cells and ratio $\kappa = p_2/p_1 = 120$.

Imperfection parameter	V_2	30°			45°			75°		
		p22/p1	p12/p1	p11/p1	p22/p1	p12/p1	p11/p1	p22/p1	p12/p1	p11/p1
$K = 10^{-5}$	0.1	0.83057	−0.00796	0.80301	0.82133	−0.00327	0.81480	0.81793	0.00093	0.81843
	0.2	0.70460	−0.02737	0.60981	0.67685	−0.01101	0.65483	0.66574	0.00311	0.66741
	0.3	0.60400	−0.05521	0.41273	0.55704	−0.02122	0.51460	0.53633	0.00597	0.53953
	0.4	0.51524	−0.09982	0.16946	0.45510	−0.03297	0.38916	0.42429	0.00912	0.42917
$K = 10$	0.1	1.18900	−0.00737	1.16348	1.17811	−0.00303	1.17206	1.17476	0.00086	1.17522
	0.2	1.46072	−0.03648	1.33436	1.39927	−0.01458	1.37011	1.38250	0.00412	1.38471
	0.3	1.89708	−0.10881	1.52014	1.68249	−0.04042	1.60164	1.63390	0.01136	1.63999
	0.4	2.77979	−0.29877	1.74482	2.06150	−0.09146	1.87857	1.94536	0.02531	1.95892
$K = 10^{10}$	0.1	1.24053	−0.01150	1.20070	1.22306	−0.00471	1.21365	1.21780	0.00133	1.21852
	0.2	1.62610	−0.06111	1.41441	1.51608	−0.02383	1.46841	1.48816	0.00672	1.49176
	0.3	2.39617	−0.21174	1.66268	1.92172	−0.07065	1.78042	1.83374	0.01968	1.84428
	0.4	5.97898	−1.11151	2.12859	2.53343	−0.17671	2.18002	2.29477	0.04739	2.32016

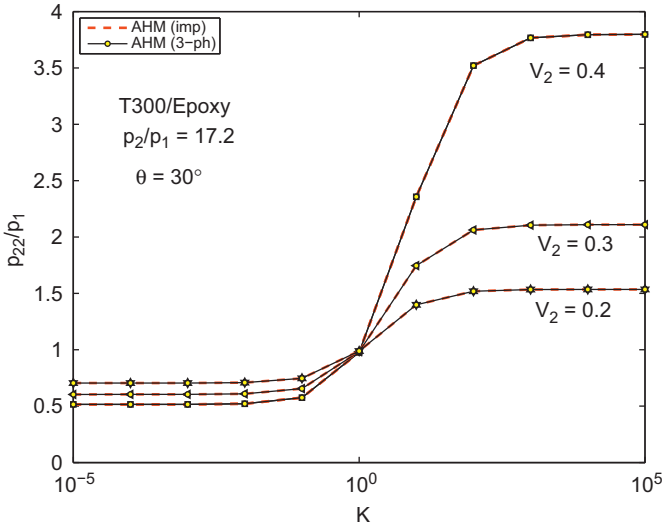

Fig. 5. The effect of elastic interface imperfection on shear dimensionless effective coefficient p_{11}/p_1 for an anisotropic composite T300 fibers and epoxy matrix for different fiber volume fraction.

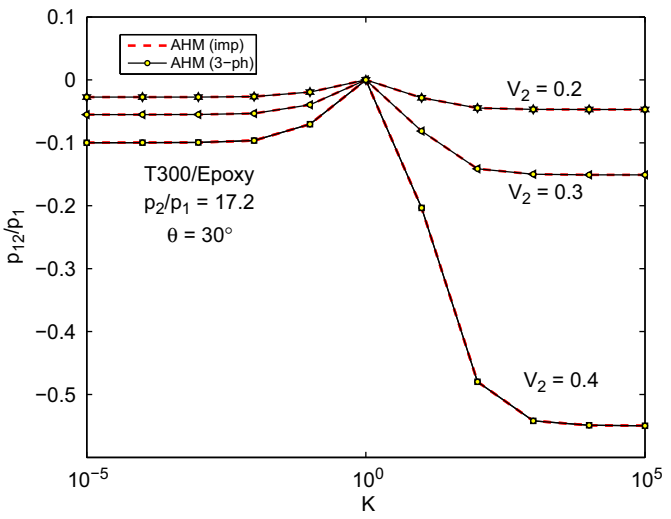

Fig. 6. The effect of elastic interface imperfection on shear dimensionless effective coefficient p_{12}/p_1 for an anisotropic composite T300 fibers and epoxy matrix for different fiber volume fraction.

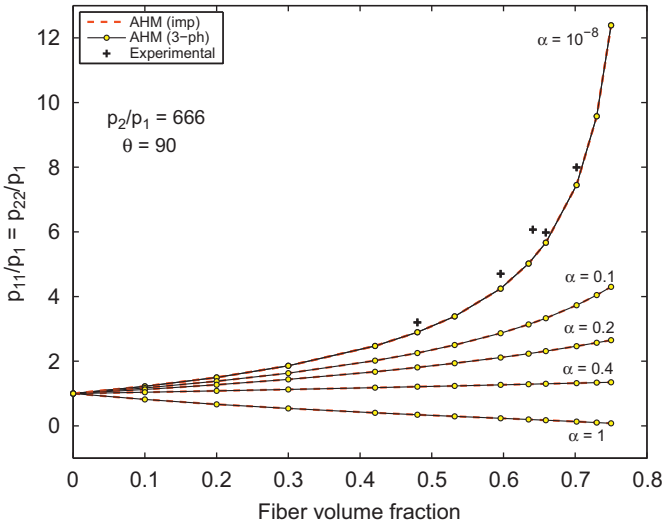

Fig. 7. Comparison between the three-phase Eqs. (44)–(47) and the spring model for imperfect contact Eqs. (36)–(39) for different imperfect parameters α, square periodic cell and ratio $\kappa=666$ with the existing experimental data (the cross symbols), taking from Zou et al. [32], for perfect interface.

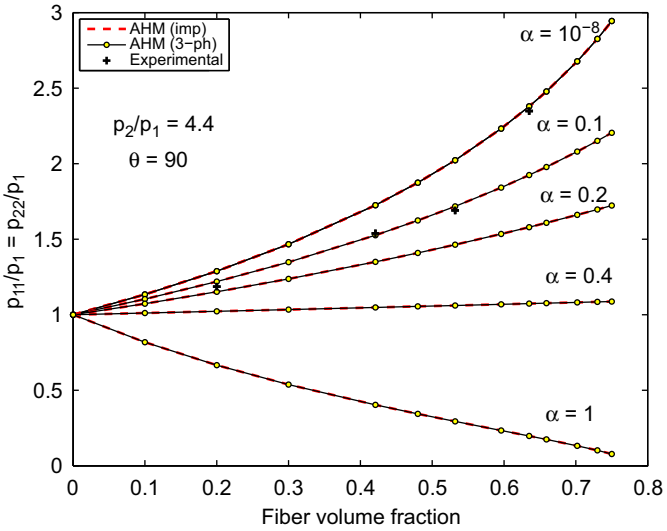

Fig. 8. Comparison between the three-phase Eqs. (44)–(47) and the spring model for imperfect contact Eqs. (36)–(39) for different imperfect parameters α, square periodic cell and ratio $\kappa=4.4$ with the existing experimental data (the cross symbols), taking from Zou et al. [32], for perfect interface.

Fig. 6 shows the coefficient p_{12}/p_1 which is negative for all the K values with the exception of $K=1$ where it almost becomes zero. The most pronounced contrast is evident for the highest volume fraction where the property considerably increases in absolute value as $K\to\infty$.

(3) As it is well known, transport property may be of both mechanical and thermal conductivity nature. Figs. 7 and 8 show the effective thermal conductivities of unidirectional fiber composites with square periodic cell with different thermal barrier giving by the parameter α. Only one effective property is studied because the composite is isotropic and $p_{11}/p_1=p_{22}/p_1$, $p_{12}/p_1=0$. The effective thermal conductivities for different values of imperfect parameter are analogously presented to those reported in Fig. 4 by Andrianov et al. [24]. A comparison between the three-phase (44)–(47) and the spring models for imperfect contact (36)–(39) is shown for periodic cell with $\theta=90^\circ$ and the two ratios $p_2/p_1=666$ and $p_2/p_1=4.4$. The non-dimensional debonding parameter α, $0\le\alpha\le1$ can be introduced as follows $K=(1-\alpha)/\alpha$, where $\alpha=0$ denotes the perfect contact between the phases and $\alpha=1$ represents the complete separation in the composite. Figs. 7 and 8 compare the present analytical predictions from Eqs. (36)–(39) and (44)–(47) with the existing experimental data (the cross symbols), taking from Zou et al. [37] for perfect interface ($\alpha=0$). Very good coincidence between these models for different values of α in the whole range of fiber volume fraction can be observed. The effective property p_{11}/p_1 become weaker in comparison with perfect contact $\alpha=0$, as a consequence of the imperfectly bonded matrix with fibers. It is seen from Fig. 7 that a good agreement between the present analytical models and experimental data is found, for a composite without tiny thermal barrier ($\alpha=10^{-8}$). This

situation can be considered as a perfect case. It is worth pointing out that in Fig. 8, when a proper thermal resistance or barrier is considered or equation ($\alpha \neq 0$), an excellent agreement between the present analytical expressions and the existing experimental data can be obtained for $\alpha = 0.1$. This means that a proper thermal barrier should be included in a theoretical model for a more accurate prediction of real thermal conductivities. Similar analysis is presented in Fig. 4 of Zou et al. [37].

(4) Table 2 shows the problem of the doubly periodic voids. Letting the inclusion and the matrix moduli be $p_2 = 10^{-5}$ GPa and $p_1 = 30$ GPa, the present method provides the results for solids with doubly periodic tunnel voids. The variation of the effective longitudinal shear modulus p_{11} for complete debond $K = 10^{-5}$ for hexagonal and square arrays are shown. Identical values to those reported in Table 7 by Jiang et al. [10] for void volume fraction are obtained. A material weakened by square or hexagonal array of tunnel voids is transversely isotropic. The effective longitudinal shear modulus of a solid with voids in a hexagonal array is higher than that with voids in a square array for the same voids volume fraction. This result is contrary to the situation of hard inclusions-soft matrix composite as it was observed by Jiang et al. [10] in Table 2.

(5) In addition, Rocha and Cruz [38] reported numerical calculations of the effective thermal conductivity of unidirectional fibrous composite materials with an interfacial thermal resistance ($1/h$) between the continuous and dispersed components. They developed a continuous variational formulation of the heat conduction problem and then applied the method of homogenization to derive the appropriate cell problem. The cell problem is solved using the finite element method (FEM). Based on the previous experimental work, Rocha and Cruz [38] defined the reference Biot number $Bi_r = hd_r/p_1$, where d_r is a typical real fiber diameter and Bi_r expresses the changes in the interfacial conductance.

In Table 3, we present a comparison between the results of the present model and FEM reported by Rocha and Cruz [38], for the effective conductivity of the hexagonal-array composite for different volume fractions and different reference Biot numbers. The conductivity ratio is considered to be $\kappa = 50$.

Table 2
Variation of the effective longitudinal shear modulus $p_{11} = p_{22}$ for complete debond $K = 10^{-5}$ for hexagonal and square arrays with the porosity. The same values that those reported in Table 7 by Jiang et al. [10] for void volume fraction with $p_1 = 30$ GPa are obtained.

Imperfection parameter	V_2	Effective coefficient	
		Hexagonal	Square
$K = 10^{-5}$	0.1	24.5455	24.5453
	0.2	20.0000	19.9959
	0.3	16.1533	16.1274
	0.4	12.8534	12.7605
	0.5	9.98427	9.73963
	0.6	7.45029	6.90954

Table 3
Comparison between the results by the AHM imperfect model and FEM reported by Rocha and Cruz [33], for the effective conductivity of the hexagonal-array composite for different volume fractions and different reference Biot numbers.

V_2	$2K = 10^{-3}$		$2K = 10^{-1}$		$2K = 10$		$2K = 10^{3}$	
	AHM	FEM	AHM	FEM	AHM	FEM	AHM	FEM
0.1	0.818347	0.81837	0.834046	0.83407	1.1366	1.1366	1.21164	1.2116
0.2	0.666943	0.66698	0.693521	0.69355	1.29323	1.2932	1.47338	1.4734
0.3	0.538797	0.53884	0.572984	0.57302	1.47464	1.4746	1.80544	1.8054
0.4	0.428854	0.42889	0.468385	0.46842	1.68722	1.6871	2.24089	2.2409
0.5	0.333254	0.33329	0.376557	0.37659	1.93975	1.9397	2.83864	2.8387
0.6	0.248814	0.24884	0.294821	0.29485	2.24464	2.2446	3.71697	3.717
0.7	0.172574	0.17259	0.220632	0.22065	2.62001	2.62	5.16021	5.1604
0.8	0.100924	0.10094	0.150848	0.15086	3.09342	3.0934	8.10996	8.1108
0.9	0.018338	0.01834	0.072568	0.07256	3.70874	3.7088	21.4080	21.409

Table 4
Comparison between the results by the AHM imperfect model and FEM reported by Rocha and Cruz [33], for the effective conductivity of the square array composite, for two concentrations of fibers and two conductivity ratios.

$2K$	$V_2 = 0.3$				$V_2 = 0.75$			
	$\kappa = 2$		$\kappa = 50$		$\kappa = 2$		$\kappa = 50$	
	AHM	FEM	AHM	FEM	AHM	FEM	AHM	FEM
10^{-7}	0.53758	0.53762	0.53758	0.53762	0.0784245	0.078432	0.0784245	0.078432
10^{-5}	0.537584	0.53762	0.537584	0.53762	0.0784305	0.078438	0.0784305	0.078438
10^{-3}	0.537936	0.53797	0.537937	0.53797	0.0790224	0.07903	0.0790226	0.07903
10^{-2}	0.541128	0.54117	0.541137	0.54117	0.0843808	0.084389	0.0843946	0.084402
10^{-1}	0.571479	0.57151	0.57227	0.5723	0.135768	0.13577	0.137074	0.13708
1	0.771995	0.77202	0.815895	0.81591	0.500212	0.50022	0.586898	0.5869
10	1.1118	1.1118	1.47486	1.4748	1.30477	1.3048	2.89478	2.8948
10^{2}	1.20935	1.2093	1.76803	1.768	1.62794	1.6279	7.28674	7.2872
10^{3}	1.22097	1.2209	1.80793	1.8079	1.67166	1.6716	9.2248	9.2256
10^{5}	1.22228	1.2222	1.81248	1.8125	1.67665	1.6766	9.53226	9.5331
10^{7}	1.22229	1.2223	1.81253	1.8125	1.6767	1.6767	9.53547	9.5363
∞	1.22229	1.2223	1.81253	1.8125	1.6767	1.6767	9.53551	9.5363

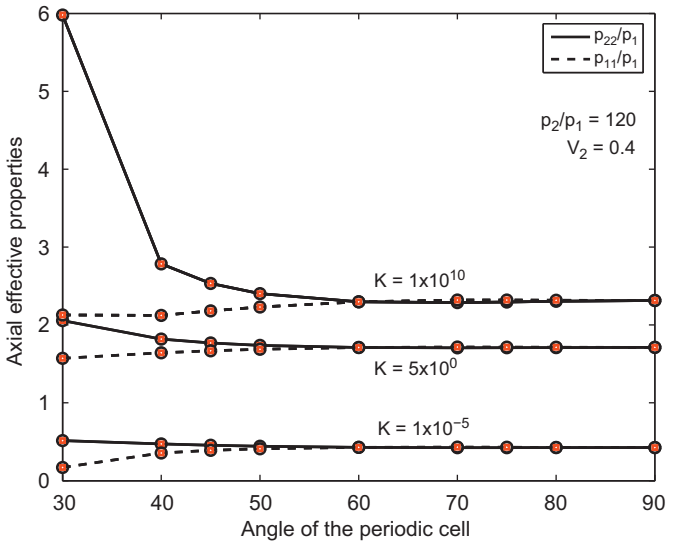

Fig. 9. Variation of the effective properties related to the angle for different values of the imperfection parameter.

The relationship between the dimensionless parameters K and Bi_r is $2K=Bi_r$. In Table 2, we can appreciate the good agreement between both models.

(6) In Table 4, we compared the results of the present model (AHM) with the calculations of Rocha and Cruz [38], for the effective conductivity of the square array composite, for two concentrations of fibers $V_2=\{0.3, 0.75\}$ and two conductivity ratios $\kappa=\{2, 50\}$. As expected physically, for fixed V_2, the effective conductivity increases as the contact conductance K increases; if the fibers are more conducting than the matrix, the effective conductivity also increases as the concentration does as well. For comparison in Table 4, a good agreement between both models is appreciated.

(7) Variation of the effective properties vs. the angle for different values of the imperfection parameter is illustrated in Fig. 9. It is remarkable that the composite is strongly anisotropic for small values of the angle of the periodic cell. In this figure, AHM imperfect is represented with circles, AHM(3f) with red squares, p_{22} with a continuous line and p_{11} with discontinuous line.

9. Conclusions

Two approaches for simulation of the imperfect bonding in elastic composite materials with oblique angle of the fiber are proposed. We introduce a set of elastic *springs* between the matrix and inclusions that transmits a load from the matrix to the inclusion; the transmission stress is proportional to the displacement jump across the "matrix–inclusion" interface. Moreover, a three phase model derived by the asymptotic homogenization method is considered to study the imperfection of the composites. The connection between the two mentioned models is studied and the relations between their physical magnitudes are given in Eq. (48) for the calculations. Simple analytical expressions (36)–(39) and (44)–(47) of the shear moduli for the two approaches are given and they show the anisotropic response of the composite. In the asymptotic limit, we can simulate different degrees of the interface's response: (i) the case of the perfect bonding and (ii) the case of the complete separation of the matrix and inclusions. The imperfect interface and the angle of inclination of the fibers play an important role in the global behavior of the composite. The accuracies of the solutions were tested with other theoretical models and experimental data and good agreement were observed. These models can be extended to more complex composites in order to predict the overall properties in the design and manufacturing of one-directional fibrous composite materials.

Acknowledgements

This work was supported by the Program of Academic Stays 2009. Defects in sensors and dynamic of magnetic-electro-elastic composite. CoNaCyT-México. Thanks to Departamento de Matemáticas y Mecánica IIMAS-UNAM for their support and Ramiro Chávez Tovar and Ana Pérez Arteaga for computational assistance. This work was partially written while RRR visiting the Institute of Mechanics at University of Magdeburg, Germany. Thanks to Dr. Harald Berger for the numerical codes by FEM used in the internal checking and his valuable suggestions and comments.

References

[1] Hashin Z. Thin interphase/imperfect interface in elasticity with application to coated fiber composites. J Mech Phys Solids 2002;50:2509–37.
[2] Guinovart-Diaz R, Rodriguez-Ramos R, Bravo-Castillero J, Sabina FJ, Maugin GA. Closed-form thermo-elastic moduli of a periodic three-phase fiber-reinforced composite. J Thermal Stresses 2005;28:1067–93.
[3] Benveniste Y, Miloh T. Imperfect soft and stiff interfaces in two dimensional elasticity. Mech Mater 2001;33:309–23.
[4] Achenbach JD, Zhu H. Effect of interphases on micro and macro mechanical behavior of hexagonal-array fiber composites. J Appl Mech 1990;57:956–63.
[5] Hashin Z. Thermoelastic properties of fiber composites with imperfect interface. Mech Mater 1990;8:333–8.
[6] Hashin Z. The spherical inclusion with imperfect interface. J Appl Mech 1991;58:444–9.
[7] Hashin Z. Thermoelastic properties of particulate composites with imperfect interface. J Mech Phys Solids 1991;39:745–62.
[8] Molkov BA, Pobedria BE. Effective characteristic of fibrous unidirectional composite with periodic structure. Mech Solids 1985;No. 2:119–29. in Russian.
[9] Abolfathi N, Abhay N, Ghodrat K, Chad U. A micromechanical characterization of angular bidirectional fibrous composites. Comput Mater Sci 2008;43:1193–206.
[10] Jiang CP, Xu YL, Cheung YK, Lo SH. A rigorous analytical method for doubly periodic cylindrical inclusions under longitudinal shear and its application. Mech Mater 2004;36:225–37.
[11] Rodríguez-Ramos R, Yan P, López-Realpozo JC, Guinovart-Díaz R, Bravo-Castillero J, Sabina FJ, et al. Two analytical models for the study of periodic fibrous elastic composite with different unit cells. Compos Struct 2011;93:709–14.
[12] Guinovart-Díaz R, López-Realpozo JC, Rodríguez-Ramos R, Bravo-Castillero J, Ramirez M, Camacho-Montes H, et al. Influence of parallelogram cells in the axial behaviour of fibrous composite. Int J Eng Sci 2010;49:75–84.
[13] Ghahremani F. Effect of grain boundary sliding on anelasticity of polycrystals. Int J Solids Struct 1980;16:825–45.
[14] Mura T, Furuhashi R. The elastic inclusion with a sliding interface. J Appl Mech 1984;51:308–10.
[15] Mura T, Jasiuk I, Tuschida B. The stress field of a sliding inclusion. Int J Solids Struct 1985;21:1165–79.
[16] Jasiuk I, Tsuchida E, Mura T. The sliding inclusion under shear. Int J Solids Struct 1987;23:1373–85.
[17] Jasiuk I, Chen J, Thorpe MF. Elastic moduli of composites with rigid sliding inclusions. J Mech Phys Solids 1992;40:373–91.
[18] Huang J, Furuhashi R, Mura T. Frictional sliding inclusions. J Mech Phys Solids 1993;41:247–65.
[19] Gao Z. A circular inclusion with imperfect interface: Eshelby's tensor and related problems. J Appl Mech 1995;62:860–6.
[20] Zhong Z, Meguid SA. On the elastic field of a spherical inhomogeneity with an imperfectly bonded interface. J Elast 1997;46:91–113.
[21] Goland M, Reissner E. The stresses in cemented joints. J Appl Mech 1944;11:17–27.
[22] Molkov BA, Pobedria BE. Effective elastic properties of a composite with elastic contact. Izvestia Akad Nauk SSR. Mekanika Tverdovo Tela 1988;1:111–7. in Russian.
[23] Mahiou H, Beakou A. Modelling of interfacial effects on the mechanical properties of fibre-reinforced composites. Composites Part A 1998;29A:1035–48.
[24] Andrianov IV, Bolshakov VI, Danishevśkyy VV, Weichert D. Asymptotic simulation of imperfect bonding in periodic fibre-reinforced composite materials under axial shear. Int J Mech Sci 2007;49:1344–54.

[25] Needleman AA. Continuum model for void nucleation by inclusion debonding. J Appl Mech 1987;54:525–31.
[26] Needleman AA. Micromechanical modelling of interfacial decohesion. Ultramicroscopy 1992;40:203–14.
[27] Levy AJ, Dong Z. Effective transverse response of fiber composites with nonlinear interface. J Mech Phys Solids 1998;46:1279–300.
[28] Levy. AJ. The fiber composite with nonlinear interface—part I: axial tension. J Appl Mech 2000;67:727–32.
[29] Levy. AJ. The fiber composite with nonlinear interface—part II: antiplane shear. J Appl Mech 2000;67:733–9.
[30] Pobedrya BE. Mechanics of composite materials. Moscow: Moscow State University Press; 1984. in Russian.
[31] Camacho-Montes H, Sabina FJ, Bravo-Castillero J, Guinovart-Díaz R, Rodríguez-Ramos R. Magnetoelectric coupling and cross-property connections in a square array of a binary composite. Int J Eng Sci 2009;47:294–312.
[32] López-López E, Sabina FJ, Bravo-Castillero J, Guinovart-Díaz R, Rodríguez-Ramos R. Overall electromechanical properties of a binary composite with 622 symmetry constituents. Antiplane shear piezoelectric state. Int J Solids Struct 2005;42:5765–77.
[33] Bakhvalov N, Panasenko G. Homogenisation: averaging processes in periodic media. Dordrecht: Kluwer; 1989.
[34] Muskhelishvili NI. Some Basic Problems in the Mathematical Theory of Elasticity. Noordhoff. Groningen; 1953.
[35] Rodriguez-Ramos R, Sabina FJ, Guinovart-Díaz R, Bravo-Castillero J. Closed-form expressions for the effective coefficients of fibre-reinforced composite with transversely isotropic constituents-I. Elastic and square symmetry. Mech Mater 2001;33:223–35.
[36] Guinovart-Diaz R, Bravo-Castillero J, Rodríguez-Ramos R, Sabina FJ. Closed-form expressions for the effective coefficients of fibre-reinforced composite with transversely isotropic constituents-I. Elastic and hexagonal symmetry. J Mech Phys Solids 2001;49:1445–62.
[37] Zou M, Yu B, Zhang D. An analytical solution for transverse thermal conductivities of unidirectional fibre composites with thermal barrier. J Phys D: Appl Phys 2002;35:1867–74.
[38] Rocha RPA, Cruz ME. Computation of the effective conductivity of unidirectional fibrous composite with an interfacial thermal resistance. Numer Heat Transfer, Part A 2010;39:179–203.